Vinyl Ester Resin: Rheological Behaviors, Curing Kinetics, Thermomechanical, and Tensile Properties

Xi Zhang, Vahid Bitaraf, Suying Wei, and Zhanhu Guo
Dan F Smith Dept. of Chemical Engineering, Integrated Composites Laboratory (ICL), Lamar University, Beaumont, TX 77710

Xi Zhang and Suying Wei
Dept. of Chemistry and Biochemistry, Lamar University, Beaumont, TX 77710

Henry A. Colorado
Dept. of Mechanical and Aerospace Engineering, University of California Los Angeles, Los Angeles, CA 90095

DOI 10.1002/aic.14277
Published online November 18, 2013 in Wiley Online Library (wileyonlinelibrary.com)

The effects of isothermal temperature on the curing extent, gel time, dynamic rheological behaviors, and mechanical properties of vinyl ester resins (VERs) were systematically studied. Although, the curing extent was observed increase with increasing the operating temperature, the study of residual heat of cured VERs indicated that the final curing extent depended on the postcuring process. The values of shear storage and loss modulii at gel point were observed to decrease with increasing both the isothermal temperature and heating rate, which were associated with the formation of microgels during the gelation process. With increasing isothermal temperature and heating rate, the microgel did not have enough time to grow well, causing a reduced shear storage and loss modulii at the gel time. The storage and loss modulii of the cured VERs were also studied and shown that with temperature increased to the glass transition, both modulii were first decreased and then increased. © 2013 American Institute of Chemical Engineers *AIChE J*, 60: 266–274, 2014

Keywords: vinyl ester resin, curing extent, kinetic study, rheological behaviors, thermomechanical properties, tensile mechanical properties

Introduction

The development of vinyl ester resins (VERs) has attracted more interests due to their unique physicochemical properties, which combined the properties of polyester and epoxy resins together.[1] The cured resins show advantages such as high resistance to the moisture and chemicals[2] and good mechanical properties.[3] Due to the outstanding properties, VERs are widely used in industrial fields, for instance, VERs can be used to replace polyester in marine, owing to its higher heat-distortion and better water resistance,[4] and VERs can serve as a matrix for composite fabrication.[5]

Although, as a thermosetting polymer, VERs could be easily prepared by curing at room temperature and normal pressure, the curing process was reported to strongly depend on curing temperature, initiators, and accelerator levels and so forth. The isothermal curing kinetic of VERs has been widely studied by differential scanning calorimetry (DSC),[6] fourier transform infrared, thermal scanning rheometry (TSR),[7] and dynamic-mechanical thermal analysis.[8] For the isothermal curing process with the polymerization proceeding, the reaction rate would sharply increase and then reached a plateau,[9] and the conversion increased with increasing isothermal temperature, for instance, the conversion of isothermal polymerization of photoinitiated VERs was studied and it was observed that the isothermal conversion increased from 22% for −30°C to 89% for 90°C.[6] The effect of isotheraml temperature on the gelation process of VERs was also studied, and the vitrification of VERs was observed to depend on the isothermal temperature. The gel time as a function of isothermal curing temperature of VERs was studied by isothermal TSR, the results have shown that increasing isothermal temperature replace leaded with led to an enhanced mobility of the active chains, which further caused a decreased gel time.[7] In addition, the reaction orders of the radical polymerization at various isothermal temperature were also calculated and observed to decrease with increasing temperature.[9] However, most of the kinetic studies on isothermally cured VER are focused on the conversion, and its effect on the mechanical properties has been rarely reported. In addition, limited discussion can be found about the effect of postcuring process on the curing extent, which is a very important for industry field application.

In this article, VERs at various isothermal temperatures were prepared by isothermally curing for 4 h followed by postcuring at 85°C for 0.5 h. The effects of isothermal temperature and postcuring process on the curing extent were studied. And the dynamic rheological behaviors of the

Correspondence concerning this article should be addressed to Z. Guo at zhanhu.guo@lamar.edu and S. Wei at suying.wei@lamar.edu.

uncured samples (liquid phase), including shear storage, and loss modulii were investigated. The effects of isothermal temperature on the gel time and the gel temperature were systematically studied as well. And for all the cured samples (solid phase), the mechanical properties including storage and loss modulii, glass transition temperature, tensile strength, and Young's modulus were evaluated together with the curing extent of the VERs.

Experimental

Materials

The polymeric matrix used was VER, Derakane momentum 411–350 (manufactured by the Dow Chemical Company), which is a mixture of 55 wt% vinyl ester with an average molecule weight of 970 g/mole and 45 wt% styrene monomers. Styrene with only one unsaturated carbon–carbon double bond provides linear chain extension. Vinyl ester monomers with two reactive vinyl end groups enable the cross-linking for network formation. The liquid resin has a density of 1.045 g/cm^3 and a viscosity of 350 centipoises (cps) at room temperature. Methyl ethyl ketone peroxide (MEKP) (curing catalyst or initiator, organic peroxide, liquid) was purchased from Miller-Stephenson Chemical Company. All the chemicals were used as-received without any further treatment.

Preparation of cured VER

The monomer and catalyst were mechanically stirred at room temperature for 5 min, and then the solution was poured into silicone rubber molds and cured isothermally at 20, 40, 60, and 80°C for 4 h and then increased the temperature to 85°C for half hour to accomplish the postcuring process. Finally, the mixtures were cooled down naturally to room temperature. VERs were isothermally cured at different temperatures to study the effect of the curing temperature on the properties of the cured resins.

Characterizations

Thermal Characterization of Epoxy Nanocomposites. Differential scanning calorimeter (DSC, TA Instruments Q2000) measurements were implemented under a nitrogen flow rate of approximately 20 mL/min at a heating rate of 10°C/min from 40 to 300°C, and for isothermally cured, the test was set as the isothermal for 240 min.

Dynamic Rheological Behaviors of Uncured VER. Dynamic rheological measurements were performed both isothermally and nonisothermally by using an environmental test chamber aluminum parallel-plate geometry (25 mm in diameter). For the isothermally test, shear storage and loss mudulii were obtained by operating the measurement isothermally at 20, 40, 60, and 80°C with a sweeping time range between 0 and 700 s at a low strain (1%) in a rheometer (AR 2000ex, TA Instrumental Company). For the nonisothermally test, the shear storage and loss mudulii were measured at different temperature ramp rate (0.5, 1, 2, 5°C/s).

Mechanical Characterization of Isothermally Cured VER. Dynamic mechanical analyses (DMA) measurements were carried out in the torsion rectangular mode using an AR 2000ex (TA Instrumental Company) with a strain of 0.05%, a constant frequency of 1 Hz and a heating rate of 2°C/min in the temperature range of 30–200°C. The sample dimensions were $12 \times 3 \times 40$ mm^3.

Tensile tests were carried out following ASTM (Standard D 412-98a, 2002) in a unidirectional tensile testing machine (ADMET tensile strength testing system). The parameters (displacement and load) were controlled by a digital controller (MTEST Quattro) with MTESTQuattro Materials Testing Software. The samples were prepared as described for the nanocomposite fabrication in silicone rubber molds, which were designed according to the standard ASTM requirement. A crosshead speed of 1.00 mm/min was used and the strain (mm/mm) was calculated by dividing the crosshead displacement by the original gauge length.

Morphological Characterizations of Isothermally Cured VER. After the tensile test, the broken samples were collected and the morphology of the fracture surfaces was characterized with a field emission scanning electron microscope (SEM, Hitachi S-3400 scanning electron microscopy). Before testing, the samples were first coated with a thin gold layer for better imaging.

Theoretical background

The free radical polymerization reaction contains the initiation, propagation, and termination three steps. $R^\bullet$ is the free redical, M is monomer, $M_x^\bullet$ and $M_y^\bullet$ are polymer chain with active ends. R_i is the reaction rate of initiation, f is initiation efficient, k_d is the rate constant of initiator dissociation, $[I]$ is the concentration of free radical, R_p is the reaction rate of propagation, k_p is the rate constant of propagation, $[M]$ is the concentration of monomer, $[M^\bullet]$ is the concentration of polymer chain with active ends, R_t is the reaction rate of termination, and k_t is the rate constant of termination.

$$R^\bullet + M \rightarrow RM^\bullet \tag{a}$$

First, the monomer is initiated by the free radicals as reaction (a), and the reaction rate is calculated as Eq. 1

$$R_i = 2fk_d[I] \tag{1}$$

$$RM^\bullet \xrightarrow{+M} RM_2^\bullet \xrightarrow{+M} RM_3^\bullet \xrightarrow{+M} \cdots RM_x^\bullet \tag{b}$$

The segment with active end will further react with other monomers and form polymer chain, which is the propagation of polymer chain, reaction (b). And the reaction rate is calculated as Eq. 2

$$R_p = k_p[M][M^\bullet] \tag{2}$$

$$M_x^\bullet + M_y^\bullet \rightarrow M_x + M_y \tag{c}$$

Two polymer chains with active end would react, reaction (c), leading to the termination step. The reaction rate is calculated as Eq. b

$$R_\mathrm{t} = 2k_\mathrm{t}[M^\bullet]^2 \tag{3}$$

$$R_i = R_\mathrm{t}$$

When the reaction rate of initiation and termination the system reach equilibrium, and replace R_t with Eq. b, the concentration of polymer chain with active end can be calculated by Eq. 4

$$[M^\bullet] = \left(\frac{R_i}{2k_\mathrm{t}}\right)^{1/2} \tag{4}$$

And since the reaction rate of propagation is much larger than that of initiation and termination, the reaction rate of polymerization can be represented by the reaction rate of propagation,[10] thus the reaction rate of polymerization can be calculated by Eq. 5

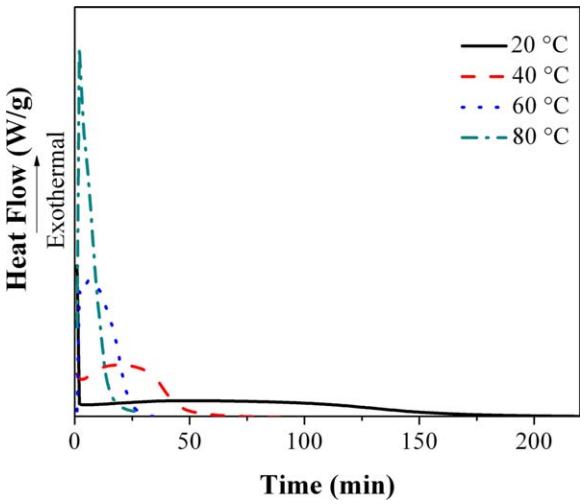

Figure 1. DSC curves of VERs isothermally cured at 20, 40, 60, and 80°C for 200 min.

[Color figure can be viewed in the online issue, which is available at wileyonlinelibrary.com.]

$$R_i \ll R_p$$
$$R = R_i + R_p = R_p$$
$$R = R_p = k_p \left(\frac{f k_d}{k_t}\right)^{1/2} [I]^{1/2}[M] \tag{5}$$

Results and Discussion

Isothermal curing of VER at different curing temperatures

The isothermal curing process of VER at different temperatures is studied by DSC test. As shown in Figure 1, the uncured VER is heated isothermally at various temperatures and the exothermal peak, which represents the curing process of VER is varied with the isothermal curing temperature. With increasing temperature, the shape of curing peak transforms from broad to sharp, which indicating that curing process would accomplish in a shorter time range at higher curing temperature. For radical polymerization, the relationship between polymerization rate constant and the temperature follows the Arrhenius law, Eq. 6[11]

$$k = Ae^{-\frac{E_a}{RT}} \tag{6}$$

where, k is the rate constant, E_a is apparent activation energy, R is the gas constant, T is the temperature, A is a pre-exponential factor. As shown in the Arrhenius law, the polymerization rate constant would increase with increasing temperature, thus at high curing temperature (80°C), the large heat flow can be observed in Figure 1.

The curing process at different temperatures is further studied by the relationship of curing extent (α) as a function of time, Figure 2. It can be clearly observed that with the isothermal curing proceeding, all samples follow the same changing trend, the curing extent first sharply increases and after reaches the maximum value, it becomes less dependent on the time and keeps constant. The existence of "saturation" curing extent is attributed to the mobility limited reaction.[12] For radical polymerization, with the reaction proceeding, the viscosity would increase and the mobility of the system, including monomers, radicals and the chains with active end, is reduced.[13] However, compared with radicals and monomers, due to the longer length, the mobility of polymer chain with active ends is more sensitive to the variation of the viscosity of the system. And with increasing viscosity, the rearrangement of the polymer segments become much harder and leads to the reduction of the terminal rate constant. Thus, at lower conversion, the rate of bimolecular termination is limited by the diffusion of segment,[14] however, the enhanced viscosity can not affect the diffusion of monomer and radical at this stage. Thus, based on Eq. 5, the reduced k_t leads to higher reaction polymerization rate, and the conversion is sharply increased. However, with the polymerization further proceeding, at high conversion, the system becomes so viscous that the mobility of the monomer and radical would also be decreased,[12] which leads to the reduction of initiation, and the curing process turns to be diffusion controlled type.[15] Thus, at high conversion, the constant curing extent can be observed in the DSC curve. In addition, because higher temperature has larger polymerization rate constant, the "saturation" curing extent increases with increased isothermal temperature, Figure 2.

Effect of postcuring function on curing extent of VER at different curing temperatures

The curing extent of samples after half hour 85°C postcuring is further studied in Figure 3. The cured samples are reheated to be completely cured. And the value of residual heat of curing can be used to calculate the curing extent of cured VERs based on Eq. 7[3]

$$\alpha = 1 - \frac{\Delta H}{\Delta H_{uc}} \tag{7}$$

where ΔH is the residual heat of the reaction in cured resin (J/g) and ΔH_{uc} is the heat of the uncured resin, with a value of 340.6 J/g. The value of curing extent (α_{pc}) for VER cured at different temperature is calculated and summarized in Table 1. As it is shown, with increasing temperature, the α_{pc} first increases and after reaches the highest value at 40°C,

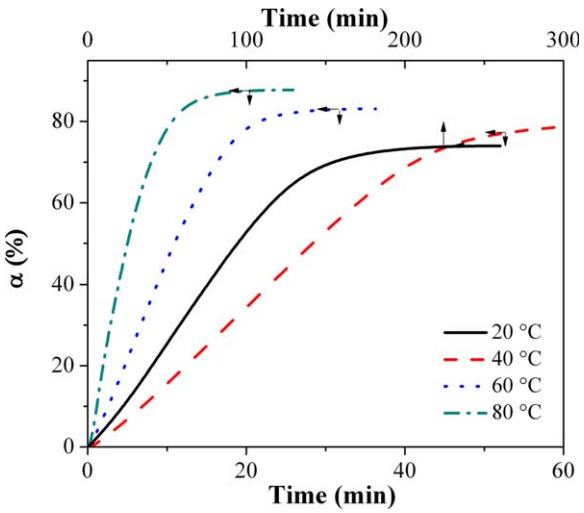

Figure 2. The experimentally obtained curing extent curves (α vs. *t*) for isothermal curing reaction of VERs at 20, 40, 60, and 80°C for 200 min.

[Color figure can be viewed in the online issue, which is available at wileyonlinelibrary.com.]

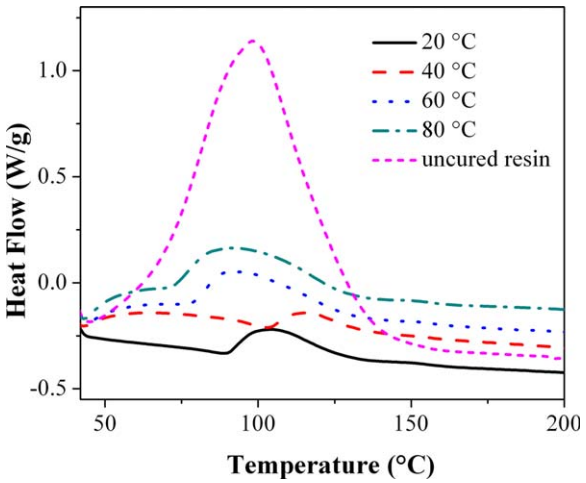

Figure 3. DSC curves of uncured VER and cured VERs at various isothermal temperature isothermally.

[Color figure can be viewed in the online issue, which is available at wileyonlinelibrary.com.]

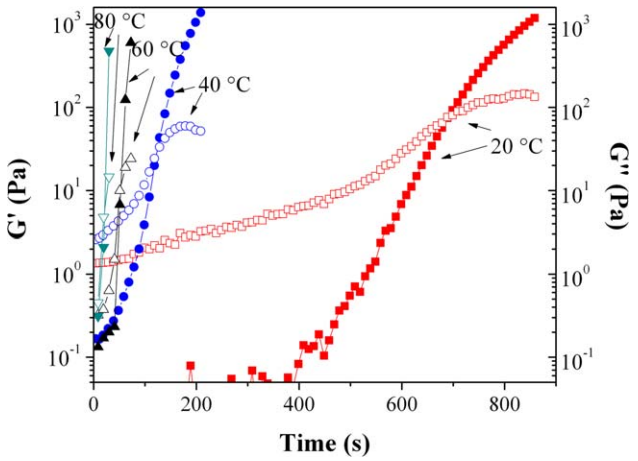

Figure 4. G′ and G″ (solid and open symbols represent G′ and G″, respectively) vs. *t* of the isothermal curing reaction of VER at various isothermal temperature.

[Color figure can be viewed in the online issue, which is available at wileyonlinelibrary.com.]

α_{pc} deceases. And compared with the α_{iso} of samples before postcuring, Figure 2, the increment extent ($\alpha_{increment}$) of the curing extent decreases with increasing isothermally curing temperature. For the isothermally cured samples, at constant temperature, the viscosity increases with increasing time, however, during the postcuting process, the temperature is increased, and the relationship between temperature and viscosity is shown in Eq. 8[16]

$$\eta = Ae^{-\frac{E_\eta}{RT}} \tag{8}$$

where, η is the rate constant, E_η is flow activation energy, R is the gas constant, and T is the temperature, A is a pre-exponential factor. Thus, with increasing temperature, the viscosity would decrease, and the reduced viscosity provides more space for the movement of radicals, monomers, and polymer chains. Thus during postcuring, the polymerization proceeds further and leads to an enhanced α. However, the reduction of viscosity would be limited with increasing the isothermal temperature, thus the lower increment of curing extent is observed in samples at higher isothermal temperature. And for samples prepared at 80°C the postcuring process caused no variation of α, which may be attributed to the aforementioned "saturation" curing extent.

Gel time and apparent activation energy (E_a)

Figure 4 shows the shear storage (G′) and loss (G″) modulus of VER as a function of time at different isothermal curing temperatures. At the very beginning of the curing process ($t = 0$ s), the VER is in liquid phase and more energy is dissipated than stored with higher G″ than G′ at this stage. With the curing process proceeding, both G′ and G″ increase and the increment of G′ is more rapid than that of G″, which is attributed to the network formation of the thermosetting materials, and at this stage the sample changes from more liquid like behavior to more solid like behavior.[17] And with cross-link density further increased, the value of G′ becomes equal to that of G″, and the corresponding time of the cross point of G′ and G″[18] is defined as gel time. And with cross-link density further increased, the value of G′ becomes equal to that of G″, and the corresponding time of the cross point of G′ and G″[19] is defined as gel time. And after reaching the gel point, the sample turns to more elasticity and more energy is stored than dissipated with G′ higher than G″ at this stage. The gel time (in molecular terms, it refers to the point, at which an infinite network is formed)[20] at different curing temperature is summarized in Table 2, and it is observed the gel time becomes shorter with increasing temperature. In addition, the apparent activation energy (E_a) can be obtained based on the relationship between the gel time and the isothermal curing temperature with Eq. 9[7,21]

$$\ln t_g = \ln t_0 + \frac{E_a}{RT} \tag{9}$$

where, t_g is gel time, E_a is apparent activation energy, R is the gas constant, T is the temperature, and t_0 is a pre-exponential factor. The relationship of $\ln t_g$ as a function of 1000/T is shown in Figure 5. The E_a value is calculated to be 50.04 KJ/mol by the fitting equation of the line, which is

Table 1. Residual Heat (ΔH, J/g), Heat Release during the Isotherml Curing Process (ΔH_{iso}, J/g), Curing Extent (α) of VERs at Different Isothermal Temperature[a]

Curing Temperature (°C)	$\Delta H(J/g)$	$\Delta H_{iso}(J/g)$	α_{pc}	α_{iso}	$\alpha_{increment}$
20	18.25	252.02	0.95	0.74	0.28
40	9.56	233.74	0.97	0.80	0.21
60	32.72	283.05	0.90	0.83	0.08
80	45.76	298.86	0.87	0.87	0.00

[a] α_{iso} and α_{pc} represent the curing extent of VER before and after postcuring respective. $\alpha_{increment}$ is the increment extent of curing extent after postcuring, $\alpha_{increment} = \frac{\alpha_{pc} - \alpha_{iso}}{\alpha_{iso}}$.

Table 2. Gel Time (t_g) of VERs at Different Isothermal Temperature

T (K)	t_g (s)
293	688.5
313	121.54
333	51.413
353	19.28

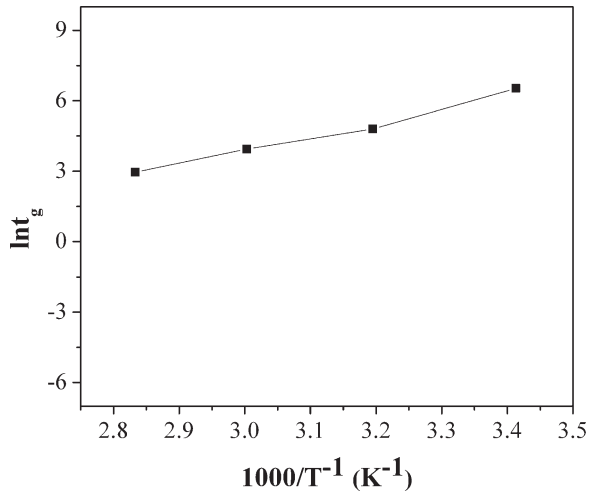

Figure 5. ln t_g vs. 1000/T^{-1} of isothermal curing reaction of VER at different isothermal temperature.

$\ln t_g = \frac{6.0187 \times 1000}{T} - 14.166$ with a fitting correlation coefficient R^2 of 0.9855. And compared with the literature reported value of 49.01 KJ/mol, the slightly difference could be associated with the different loading of MEKP.[7]

The gel time under nonisothermal conditions is also studied by investigating the shear storage (G′) and loss (G″) modulus of VER at different heating rates, Figure 6. The gel time and temperature are obtained based on the cross point of G′ and G″. The time-temperature transformation curve (Figure 7) shows the gel time and gel temperature at different heating rates. As shown in Figure 7, both the temperature and the time of the gelation depend on the heating rate, with increasing the heating rate, the gel time decreases, however, the corresponding temperature for reaching the gel time increases.

It is worth noting that for isothermal and nonisothermal conditions, G′ and G″ at gel point decrease with increasing temperature and heating rate, respectively. The decreased value of both modulus indicates that the crosslink density is reduced.[22] Generally, the gelation process includes microgel formation, transition, and macrogelation stages. At the microgel formation stage, polymer chains first form crosslinked coils, which are considered as "microgels," and at this stage, due to the low concentration of the microgel, the reaction among the microgel is limited. With the polymerization proceeding, the concentration of microgel is increased and the gelation enters the transition stage from microgelation to macrogelation, the active bonds on the surface of the microgels can react with monomers and other microgels to accomplish the growth of microgels and the crosslink between microgels, at this stage the formation of microgels still exists. However, when the system enters the macrogelation stage, the free radicals are mostly engaged in the crosslinking reaction between the microgels and the formation of macrogels becomes the dominant reaction. For the VER at high isothermal temperature and heating rate, although the reaction rate is enhanced, and the system can quickly enter the macrogelation stage, the reduction of crosslink density indicates that the microgels may not grow as well as microgels at low isothermal temperature and heating rate. Thus, lower value of G′ and G″ are observed at gel point, Figure 6A, B.

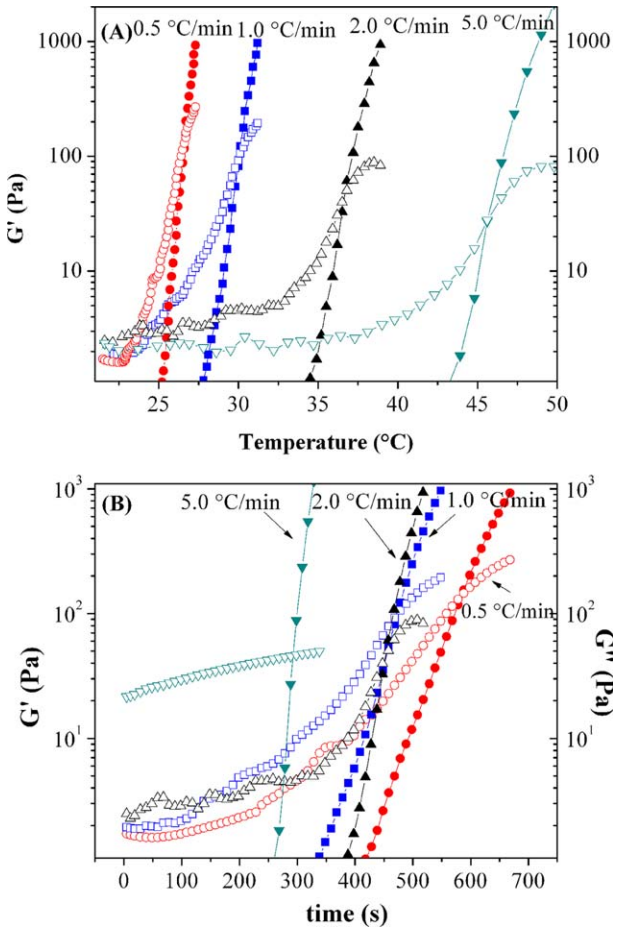

Figure 6. G′ and G″ vs. (A) temperature and (B) time of nonisothermal curing reaction of VER at different heating rates (solid and open symbol represent G′ and G″, respectively).

[Color figure can be viewed in the online issue, which is available at wileyonlinelibrary.com.]

Dynamic mechanical properties of cured VER

DMA shows information on the storage modulus (G′), loss modulus (G″) and tan δ in the test temperature range. The storage modulus represents the elastic property or the energy

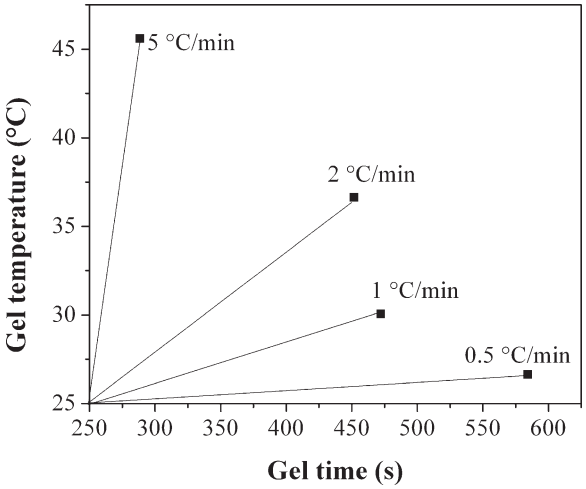

Figure 7. Time-temperature transformation curve of VER at gel point at different heating rate.

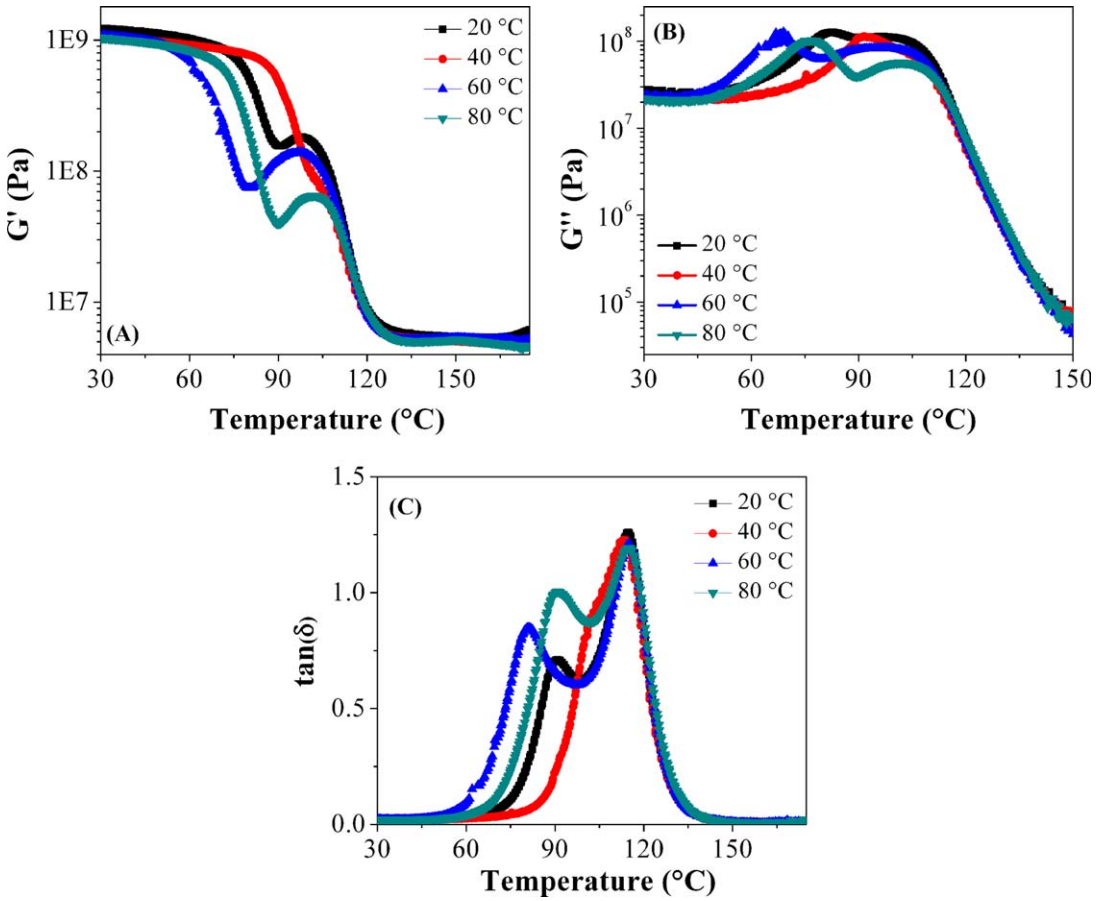

Figure 8. (A) Storage modulus (G′), (B) loss modulus (G″) and (C) tan δ vs. temperature of cured VERs at different isothermal temperature.

[Color figure can be viewed in the online issue, which is available at wileyonlinelibrary.com.]

storage in the VERs, while the loss modulus reflects the viscous behavior or the energy dissipation in the VERs during the test.[23,24] Figure 8 shows the G′ and G″ for VER at different curing temperatures. In the glass plateau (less than 60°C, when the polymer chains can not move and the values of both modulii are high), the values of both modulii are almost the same for all the samples. However, when the temperature further increases to the glass transition range of the samples (60–120°C, when the polymer chains begin to move and the modulii are sharply decreased), obvious difference is observed among the VERs at different curing temperatures. Generally, in the glass transition region, G′ would decrease with increasing temperature,[25] which is observed in the sample prepared at 40°C, Figure 8A. However, for the other samples, the G′ curves show a wave-like shape, that is, it first decreases and then increases. The unusual variation is due to the additional curing of the sample,[12] as verified the incomplete curing of VER by DSC study. During the DMA test, with temperature increasing, the samples enter the glass transition region, and sufficient molecular mobility enables further curing upon heating at high temperatures.[12] And during the further curing process, with the network formed in the resin, the movement of the polymer chains is restrained and the G′ value increases, at the same time, the network formation also causes the friction between the polymer chain enlarged, which leads to an increased G″.[26] And after the samples are well cured, as the material passing through the glass transition region and entering the rubbery region, G′ and G″ decrease with increasing temperature.[12] It is worth noting that for the sample isothermally cured at 40°C and postcured for half hour at 85°C, no unusual variation of G′ and G″ can be observed, indicating that the samples are well cured and thus no additional curing process is observed, Figure 8A, B.

The tan δ is the ratio of the loss modulus to the storage modulus, and the peak of tan δ is often used to determine the glass transition temperature, T_g. As shown in Figure 8C, there are two peaks of tan δ, as aforementioned, with increasing the temperature, the samples first enter the glass transition range, and with further increasing the temperature, additional curing takes place and after well cured, the samples would enter the glass transition again.

And since the samples are cured again and reach the same curing extent during the test, for all the samples, the second peak of tan δ overlaps together indicating the same glass transition temperature. However, the first glass transition temperature depends on the curing extent of the samples. DiBenedetto's equation can be applied to model the relationship between T_g and the curing extent, Eq. 10[27]

$$\frac{T_g - T_{gu}}{T_{gu}} = \frac{(\varepsilon_\infty/\varepsilon_0 - c_\infty/c_0)\alpha}{1-(1-c_\infty/c_0)\alpha} \tag{10}$$

where, T_{gu} is the glass transition temperature of the uncrosslinked polymer, ε is the lattice energy (the heat of sublimation of polymer from the crystalline form to gas form),[28] c is

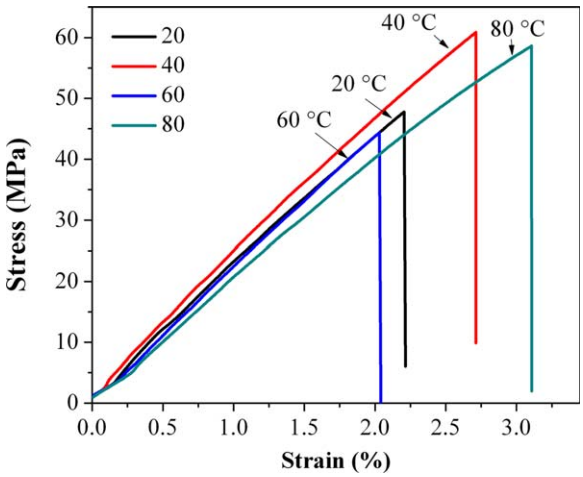

Figure 9. Tensile stress–strain curves of the cured VERs.

[Color figure can be viewed in the online issue, which is available at wileyonlinelibrary.com.]

the segmental mobility, and αis the conversion, the subindexes 0 and ∞ refer to the uncrosslined polymer and fully crosslinked polymer. Based on the DiBenedetto's equation, with increasing the conversion (curing extent), the T_g would increase. The same phenomenon is clearly shown in Figure 8C, with decreasing the curing extent, the first peak of tan δ shifts toward a low temperature range. In addition, for the highly cured sample (isothermally cured at 40°C and post-cured for half hour at 85°C, the curing extent reaches 0.97), there is only one peak shown in Figure 8C, which can be considered as the shift of first peak to a high value and overlapping with the second one.

Tensile mechanical property and fracture surface analysis of cured nanocomposites

The curves of tensile stress as a function of strain are shown in Figure 9. It can be observed that the tensile strength of the VERs depends on the curing extent (crosslinked density), with increasing crosslink density, more polymer chains are combined together, which becomes harder to be broken, thus the samples with higher curing extent show enhanced tensile strength.[29] However, VER prepared at 80°C ($\alpha_{pc} = 0.87$) shows higher elongation and tensile strength than the VERs prepared at 20°C ($\alpha_{pc} = 0.95$). The enhanced tensile strength may be attributed to shear yield initiated by the "defect" structure of the VER prepared at 80°C, as former discussed the microgels formed at high temperature may not be as good as that at low temperature, these structures may act as rubber particles in VERs, which can initiate the shear yield of the matrix.[30] Different morphologies are also observed in the SEM image of the fracture surface, Figure 10. As can be seen in Figure 10D, some shear yielding can be observed in the fracture surface, which is beneficial for the internal stress

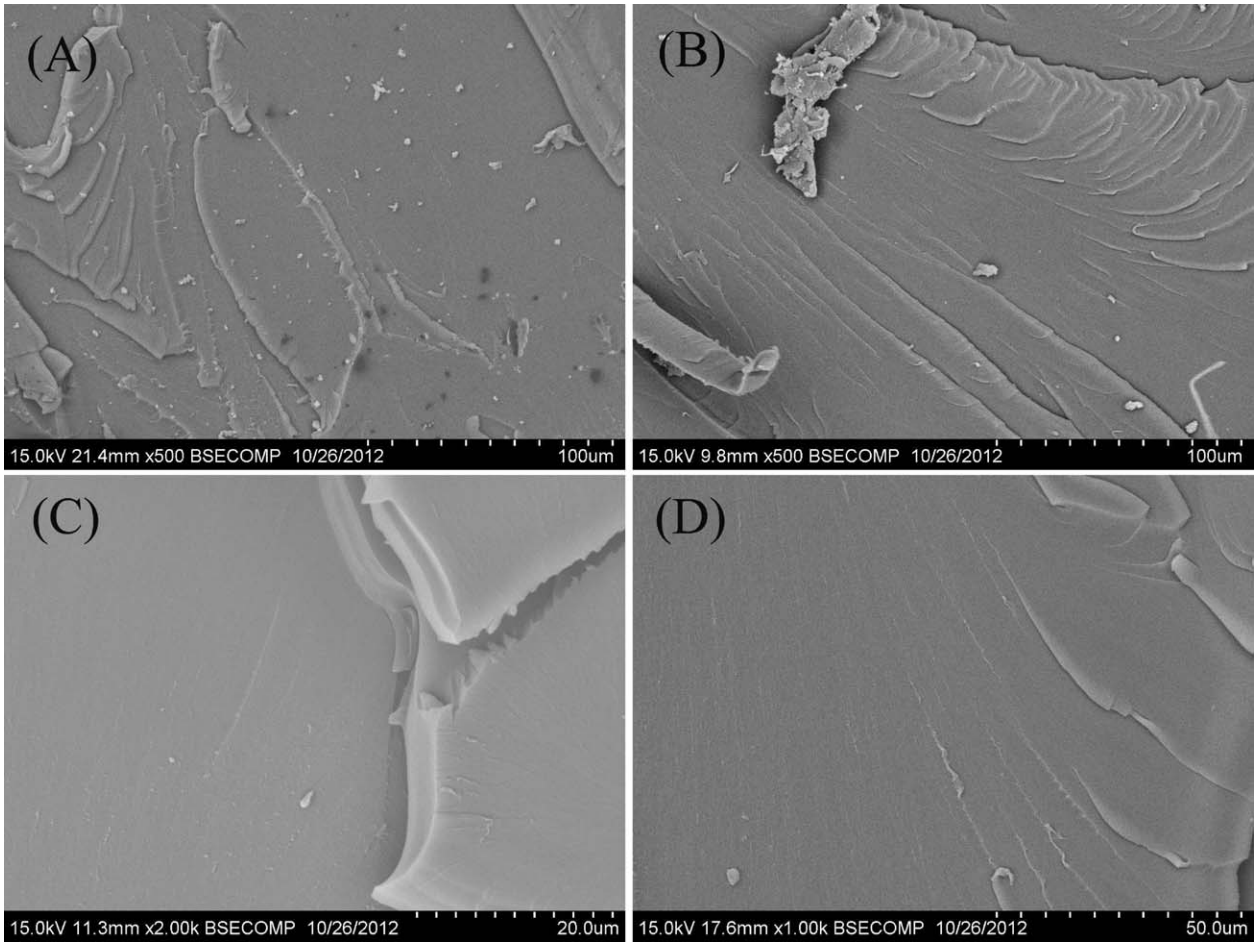

Figure 10. SEM images of fracture surface of VERs isothermally cured at (A) 20, (B) 40, (C) 60, and (D) 80°C, respectively.

transfer while an external load is applied.[31–33] The surfaces for all VERs are smooth reflecting a typical brittle fracture; however, the VER prepared with 40°C shows a rough fracture surface. A rough surface can be attributed to the polymer deformation.[23]

Conclusions

VERs at different isothermal temperatures were prepared and systematically studied. The resins were isothermally cured for 4 h followed by postcuring at 85°C for 0.5 h. The curing extent was calculated and observed increase with increasing isothermal temperature, when isothermally cured at 80°C, the curing extent of the resin can reach to 0.87. However, due to the viscosity variation with temperature, the increment of curing extent before and after postcuring decreased with increasing the isothermal temperature, and the highest α_{pc} value corresponded to the sample cured with an isothermal temperature of 40°C. The dynamic rheological behaviors, including shear storage and loss modulii of the resins were investigated and the gel time with isothermal and nonisothermal was obtained by studying the cross point of the modulii. The gel time was observed to decrease with increasing the isothermal curing temperature, and at 80°C, the resin can reach the gel point at 19.28 s. In addition, the effect of isothermal temperature on the gelation process was discussed and the value of the shear storage and loss modulii was observed to decrease with increasing isothermal temperature and heating rate at gel point. The reduction of both modulii was studied with the structure of microgels formed during gelation. With increasing isothermal temperature and heating rate, the microgel may not had enough time to grow well, which led to the reduced shear storage and loss modulii at gel time. The storage and loss modulii of cured VERs were also studied and shown that with temperature increased to the glass transition, both modulii first decreased and then increased. And two peak of tan δ were observed and the first T_g depends on the curing extent of the resin, which increased with increasing the curing extent. However, the second T_g is independent of the curing extent and all samples shown the same peak. Finally, the tensile strength of VERs was studied and the result show that the strength increased with increasing crosslinking density.

Acknowledgments

The authors appreciate the fund from National Science Foundation-Nanoscale Interdisciplinary Research Team and Materials Processing and Manufacturing (CMMI 10–30755) managed by Dr. Mary Toney for obtaining the TGA and DSC instruments. S. Wei acknowledges the Welch foundation (V-0004). H.A.C acknowledges to Universidad de Antioquia for its partial support.

Literature Cited

1. Jang C, Lacy TE, Gwaltney SR, Toghiani H, Pittman CU. Relative reactivity volume criterion for cross-linking: application to vinyl ester resin molecular dynamics simulations. *Macromolecules.* 2012; 45:4876–4885.
2. Guo Z, Lei K, Li Y, Ng HW, Prikhodko S, Hahn HT. Fabrication and characterization of iron oxide nanoparticles reinforced vinyl-ester resin nanocomposites. *Compos Sci Technol.* 2008;68:1513–1520.
3. Guo Z, Ng HW, Yee GL, Hahn HT. Differential scanning calorimetry investigation on vinyl ester resin curing process for polymer nanocomposite fabrication. *J Nanosci Nanotechnol.* 2009;9:3278–3285.
4. Mouritz AP, Mathys Z. Post-fire mechanical properties of marine polymer composites. *Compos Struct.* 1999;47:643–653.
5. Guo Z, Hahn HT, Lin H, Karki AB, Young DP. Magnetic and magnetoresistance behaviors of particulate iron/vinyl ester resin nanocomposites. *J Appl Phys.* 2008;104:014314–014315.
6. Scott TF, Cook WD, Forsythe JS. Photo-DSC cure kinetics of vinyl ester resins. I. Influence of temperature. *Polymer.* 2002;43:5839–5845.
7. Martin JS, Laza JM, Morrás ML, Rodríguez M, León LM. Study of the curing process of a vinyl ester resin by means of TSR and DMTA. *Polymer.* 2000;41:4203–4211.
8. Scott TF, Cook WD, Forsythe JS. Kinetics and network structure of thermally cured vinyl ester resins. *Eur Polym J.* 2002;38:705–716.
9. Janković B. The kinetic analysis of isothermal curing reaction of an unsaturated polyester resin: estimation of the density distribution function of the apparent activation energy. *Chem Eng J.* 2010;162: 331–340.
10. O'Brien JL, Gornick F. Chain transfer in the polymerization of methyl methacrylate. I. transfer with monomer and thiols. The mechanism of the termination reaction at 60°[1]. *J Am Chem Soc.* 1955;77: 4757–4763.
11. Lecamp L, Youssef B, Bunel C, Lebaudy P. Photoinitiated polymerization of a dimethacrylate oligomer: 2. *kinetic studies. Polymer.* 1999;40:1403–1409.
12. Cook WD, Simon GP, Burchill PJ, Lau M, Fitch TJ. Curing kinetics and thermal properties of vinyl ester resins. *J Appl Polym Sci.* 1997; 64:769–781.
13. Goodner MD, Bowman CN. Modeling primary radical termination and its effects on autoacceleration in photopolymerization kinetics. *Macromolecules.* 1999;32:6552–6559.
14. Russell GT. The kinetics of free radical polymerizing systems at low conversion, 1. On the rate determining step of the bimolecular termination reaction. *Macromol Theory Simul.* 1995;4:497–517.
15. Deng Y, Martin GC. Diffusion and diffusion-controlled kinetics during epoxy-amine cure. *Macromolecules.* 1994;27:5147–5153.
16. Saltiel J, D'Agostino JT. Separation of viscosity and temperature effects on the singlet pathway to stilbene photoisomerization. *J Am Chem Soc.* 1972;94:6445–6456.
17. Chambon F, Winter HH. Stopping of crosslinking reaction in a PDMS polymer at the gel point. *Polym Bull.* 1985;13:499–503.
18. Ilavsky M, Dusek K. Structure and elasticity of polyurethane networks. 5. Effect of diluent in the formation of model networks of poly(oxypropylene)triol and 4,4-methylenebis(phenyl isocyanate). *Macromolecules.* 1986;19(8):2139–2146.
19. Senff H, Richtering W. Temperature sensitive microgel suspensions: colloidal phase behavior and rheology of soft spheres. *J Chem Phys.* 1999;111:1705–1711.
20. Kulshreshtha AK, Vasile C. Handbook of Polymer Blends and Composites, Vol. 1. Exeter, UK: Polestar Scientifica, 2002.
21. Montserrat S, Roman F, Colomer P. Vitrification and dielectric relaxation during the isothermal curing of an epoxy-amine resin. *Polymer.* 2003;44:101–114.
22. Winter HH, Chambon F. Analysis of linear viscoelasticity of a crosslinking polymer at the gel point. *J Rheol.* 1986;30:367–382.
23. Zhu J, Wei S, Ryu J, Budhathoki M, Liang G, Guo Z. In situ stabilized carbon nanofiber (CNF) reinforced epoxy nanocomposites. *J Mater Chem.* 2010;20:4937–4948.
24. Fabry B, Maksym GN, Butler JP, Glogauer M, Navajas D, Fredberg JJ. Scaling the microrheology of living cells. *Phys Rev Lett.* 2001; 87:148102.
25. Martin O, Avérous L. Poly(lactic acid): plasticization and properties of biodegradable multiphase systems. *Polymer.* 2001;42:6209–6219.
26. Gong X, Liu J, Baskaran S, Voise RD, Young JS. Surfactant-assisted processing of carbon nanotube/polymer composites. *Chem Mater.* 2000;12:1049–1052.
27. Hale A, Macosko CW, Bair HE. Glass transition temperature as a function of conversion in thermosetting polymers. *Macromolecules.* 1991;24:2610–2621.
28. Billmeyer FW. Lattice energy of crystalline polyethylene. *J Appl Phys.* 1957;28:1114–1118.
29. Park S, Lee K-S, Bozoklu G, Cai W, Nguyen ST, Ruoff RS. Graphene oxide papers modified by divalent ions—enhancing mechanical properties via chemical cross-linking. *ACS Nano.* 2008;2:572–578.
30. Huang Y, Kinloch AJ. The role of plastic void growth in the fracture of rubber-toughened epoxy polymers. *J Mater Sci Lett.* 1992;11:484–487.

31. Zhang X, Alloul O, Zhu J, et al. Iron core carbon shell nanoparticles reinforced electrically conductive magnetic epoxy resin nanocomposites with reduced flammability. *RSC Adv*. 2013:3:9453–9464.
32. Zhang X, He Q, Gu H, Guo Z, Wei S. Polyaniline stabilized barium titanate nanoparticles reinforced epoxy nanocomposites with high dielectric permittivity and reduced flammability. *J Mater Chem C*. 2013;1:2886–2899.
33. Zhang X, He Q, Gu H, Colorado HA, Wei S, Guo Z. Flame retardant conductive epoxy resin nanocomposites reinforced with various polyaniline nanostructures. *ACS Appl Mater Interfaces*. 2013;5:898–910.

Manuscript received May 17, 2013, and revision received Sept. 6, 2013.